NeuroImage: Clinical 16 (2017) 276–285

Contents lists available at ScienceDirect

NeuroImage: Clinical

journal homepage: www.elsevier.com/locate/ynicl

Specific DTI seeding and diffusivity-analysis improve the quality and prognostic value of TMS-based deterministic DTI of the pyramidal tract☆,☆☆

Tizian Rosenstock[a,*], Davide Giampiccolo[b], Heike Schneider[a], Sophia Jutta Runge[a], Ina Bährend[a], Peter Vajkoczy[a], Thomas Picht[a]

[a] Department of Neurosurgery, Charité University Medicine, Charitéplatz 1, 10117 Berlin, Germany
[b] Institute of Neurosurgery, University Hospital, Piazzale Stefani 1, 37100 Verona, Italy

ARTICLE INFO

Keywords:
Navigated transcranial magnetic stimulation (nTMS)
Brain tumor surgery
Glioma
Motor outcome
Diffusion tensor imaging
Fractional anisotropy
Apparent diffusion coefficient

ABSTRACT

Object: Navigated transcranial magnetic stimulation (nTMS) combined with diffusion tensor imaging (DTI) is used preoperatively in patients with eloquent-located brain lesions and allows analyzing non-invasively the spatial relationship between the tumor and functional areas (e.g. the motor cortex and the corticospinal tract [CST]). In this study, we examined the diffusion parameters FA (fractional anisotropy) and ADC (apparent diffusion coefficient) within the CST in different locations and analyzed their interrater reliability and usefulness for predicting the patients' motor outcome with a precise approach of specific region of interest (ROI) seeding based on the color-coded FA-map.

Methods: Prospectively collected data of 30 patients undergoing bihemispheric nTMS mapping followed by nTMS-based DTI fiber tracking prior to surgery of motor eloquent high-grade gliomas were analyzed by 2 experienced and 1 unexperienced examiner. The following data were scrutinized for both hemispheres after tractography based on nTMS-motor positive cortical seeds and a 2nd region of interest in one layer of the caudal pons defined by the color-coded FA-map: the pre- and postoperative motor status (day of discharge und 3 months), the closest distance between the tracts and the tumor (TTD), the fractional anisotropy (FA) and the apparent diffusion coefficient (ADC). The latter as an average within the CST as well as specific values in different locations (peritumoral, mesencephal, pontine).

Results: Lower average FA-values within the affected CST as well as higher average ADC-values are significantly associated with deteriorated postoperative motor function ($p = 0.006$ and $p = 0.026$ respectively). Segmental analysis within the CST revealed that the diffusion parameters are especially disturbed on a peritumoral level and that the degree of their impairment correlates with motor deficits (FA $p = 0.065$, ADC $p = 0.007$). No significant segmental variation was seen in the healthy hemisphere. The interrater reliability showed perfect agreement for almost all analyzed parameters.

Conclusions: Adding diffusion weighted imaging derived information on the structural integrity of the nTMS-based tractography results improves the predictive power for postoperative motor outcome. Utilizing a second subcortical ROI which is specifically seeded based on the color-coded FA map increases the tracking quality of the CST independently of the examiner's experience. Further prospective studies are needed to validate the nTMS-based prediction of the patient's outcome.

1. Introduction

Navigated transcranial magnetic stimulation (nTMS) has been established as a reliable, non-invasive and safe tool for analyzing cortical motor representation and motor functionality within the scope of preoperative surgical planning for patients with motor eloquent brain lesions in a superior manner compared to fMRI (Forster et al., 2011; Forster et al., 2014; Krieg et al., 2012b; Picht et al., 2009; Tarapore et al., 2016; Zdunczyk et al., 2013). In these patients an extensive resection can lead to an increased survival and quality of life (Almenawer et al., 2015; Hervey-Jumper and Berger, 2016; Sanai and Berger, 2008) while inducing a new surgery-related functional deficit – like a paresis – needs to be avoided. Not only that a new deficit negatively affects the patient's quality of life but it also decreases the survival (McGirt et al.,

☆ Funding: We declare that no funding was received that supported the research.
☆☆ Conflict of interests: We declare no conflict of interest.
* Corresponding author.
E-mail address: tizian.rosenstock@charite.de (T. Rosenstock).

http://dx.doi.org/10.1016/j.nicl.2017.08.010
Received 19 December 2016; Received in revised form 22 June 2017; Accepted 11 August 2017
Available online 12 August 2017

2009).

The accuracy of nTMS compared with the data acquired from intraoperative neurophysiological mapping (IOM) as the gold standard for resection of rolandic brain tumors (Duffau et al., 2005; Kombos et al., 2009a) - has been recently shown (Forster et al., 2015; Picht et al., 2011; Tarapore et al., 2012). In addition, it is suggested that applying preoperative nTMS mapping leads to more extensive resections and a decreased rate of postoperative motor deficits (Frey et al., 2014; Krieg et al., 2014; Picht et al., 2016).

In case of brain tumors affecting the corticospinal tract (CST) nTMS-based fiber tracking (FT) can be used to analyze the spatial relationship between CST and presumed tumorous tissue (Frey et al., 2012; Krieg et al., 2012a; Rosenstock et al., 2016; Weiss et al., 2015). Several studies have shown that a second region of interest (ROI) increases the quality of tractography. Different procedures for placing this second ROI have been published (Conti et al., 2014; Frey et al., 2012; Krieg et al., 2012a; Weiss et al., 2015).

The aim of this study was to analyze in how far the quality of nTMS-based FT can be optimized in a user-independent and standardized manner by seeding a 2nd ROI in one layer of the caudal pons based on the color-coded fractional-anisotropy (FA) map (Mori and van Zijl, 2002) additionally to the cortical nTMS-based ROI. Furthermore, we wanted to find out to what extent the data provided by the nTMS-based FT have prognostic value in terms of postoperative motor function.

2. Methods

2.1. Ethical standard

The study proposal is in accordance with ethical standards of the Declaration of Helsinki and was approved by the Ethics Commission of the Charité University Hospital (#EA4/007/06 and #EA1/037/16). All patients provided written informed consent for medical evaluations and treatments within the scope of the study.

2.2. Patients

Patients (n = 30) presenting with high grade glioma (according to the WHO classification) (Louis et al., 2007) closely located to the motor cortex and/or the corticospinal tract (CST) between August 2011 and March 2016 were prospectively included in this study. All of them were operated after noninvasive functional motor mapping by nTMS for evaluating the possibility of safe tumor resection. Study exclusion criteria matched with the contraindications of TMS (> 1 generalized seizure or cranial implants). The patients were examined neurologically preoperatively, at the day of discharge and after 3 months by an experienced neurosurgeon. The following data were documented in a custom-made database: age, sex, antiepileptic or antiedematous medication, Karnofsky Performance Scale (KP) (Schag et al., 1984), motor status (according to the British Medical Research Council (MRC) grade where 0 means no muscle activation and 5 means full muscle strength).

2.3. MRI data

A 1.5 or 3-T MR imaging unit (GE Healthcare, Milwaukee, Wis) with an 8-channel head coil was used to perform at least a T1-weighted contrast-enhanced 3D gradient echo sequence, T2-weighted fast spin-echo sequence fluid-attenuated inversion recovery (FLAIR) sequence and diffusion tensor imaging (single-shot echo-planar sequence along 23 different geometric directions at a b-value of 1000 s/mm^2), as previously described in detail (Frey et al., 2012). All MR scans were analyzed and interpreted by an interdisciplinary board of neurosurgeons and neuroradiologists. The T1-weighted contrast-enhanced 3D gradient echo sequence was used to generate a 3D reconstruction with our nTMS system (eXimia, Nexstim Oy) for navigating the stimulation location over the cortex.

2.4. Navigated TMS mapping

Noninvasive functional motor mapping of the affected and healthy hemisphere was performed in each patient using nTMS, as specified previously (Picht et al., 2011). Briefly, the principle of electromagnetic induction is used to produce a brief, cone-shaped magnetic field by a prompt discharge of a figure-of-eight stimulation coil, which then induces an electric field in the underlying brain. Depending on the stimulation location and intensity, compound muscle action potentials will be recorded by the system's integrated electromyography (EMG) unit (sampling rate 3 kHz, resolution 0.3 mV; Neuroline 720, Ambu). Muscle activity (MEP amplitude ≥ 50 μV) is detected by surface electrodes attached to the abductor pollicis brevis and first digital interosseus (FDI) of the upper extremity in each patient and – depending on the individual tumor location – for the lower extremity to the tibialis anterior and abductor halluces brevis muscle. The mapping is performed utilizing neuronavigation where the position of the head and the coil is tracked by an infrared tracking camera (Polaris Vicra) which allows to control the stimulation location over the cortex with a navigation accuracy of lower than or equal to 2 mm.

Prospective data collection followed a highly standardized mapping protocol and following integration of nTMS-data into our surgical planning software (iPlan 3.0, BrainLab) is visualized in Fig. 1.

2.5. Fiber tracking – ROI seeding

The nTMS stimuli locations along the precentral gyrus were used as region of interest (ROI) (Fig. 1) for bihemispheric tracking of the CST based on DTI (Rosenstock et al., 2016).

In this study, all trackings were performed with a vector step length of 1.6 mm, an angular threshold of 30°, a minimum fiber length of 110 mm and 75% of the fractional anisotropy threshold (FAT) where the FAT is the highest adjusted FA value with which a fiber tracking could be performed as described previously in detail (Frey et al., 2012). The following tractography parameters were registered: number of fibers belonging to the CST, number of fibers not belonging to the CST (aberrant fibers, Fig. 2), the closest distance between tumor and CST, the occurrence of edema within the CST, the volume of the tracts as well as the fractional anisotropy (FA, measure of the directiveness of water diffusion within a voxel) and the apparent diffusion coefficient (ADC, measure of the diffusivity of water within a voxel in mm^2/s) (Basser et al., 1994) measured within the CST where both values were noted as A) average values and B) local values in different locations (“cortical” = most cranial part of the CST, peritumoral, mesencephal, pontine).

We compared the tracking results following 2 different approaches of subcortical ROI seeding: A) conventional cubic ROI in the anterior inferior pons – seeded by anatomical landmarks/knowledge (Weiss et al., 2015) and B) specific plane ROI in one layer of the caudal pons defined by the color-coded FA-map (Fig. 1).

2.6. Fiber tracking with specific (color-coded, 2-dimensional) ROI

Varying values of adjusted FA values can lead to varying tracking results where the ROIs' location highly influences them, reflecting differences in local FA values (Frey et al., 2012; Negwer et al., 2016; Negwer et al., 2017; Weiss et al., 2015). Therefore we analyzed tractography results performed with the specific plane ROI and different FA values (0.01, 0.05, 0.1, 25% of FAT, 50% of FAT and 75% of FAT) in terms of plausibility and tractography parameters described above to identify the optimal tracking algorithm for the preoperative evaluation. Moreover, the FTs of the CST based on the specific plane ROI were reproduced for interrater reliability analysis using the 75% of FAT protocol (Fig. 1) by one experienced examiner (> 50 fiber trackings performed before) and one totally unexperienced examiner (no contact to preoperative planning procedure before).

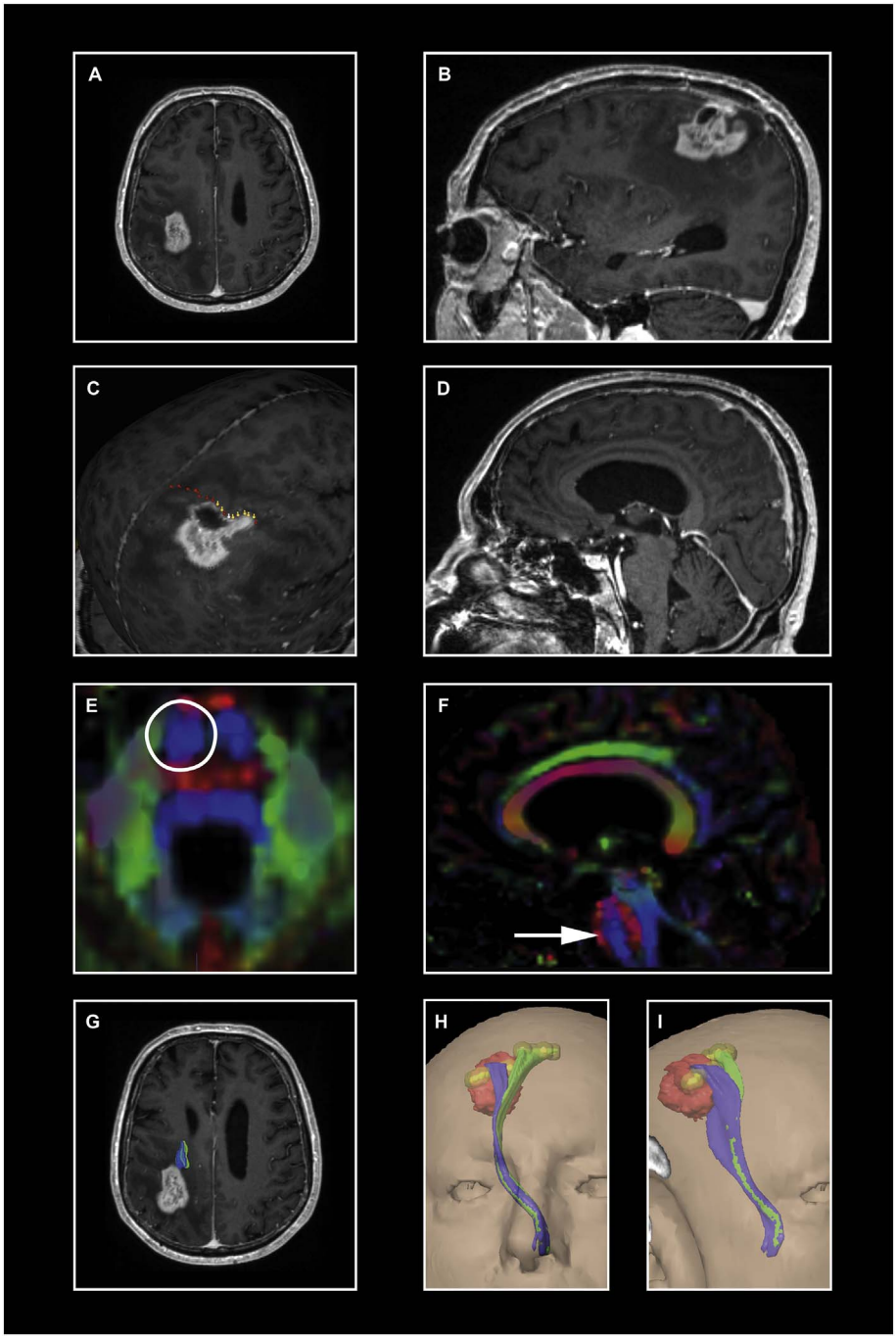

Fig. 1. Illustration of our highly standardized protocol. A patient with a (post)central glioma (WHO IV°) is presented (A, B). Navigated TMS stimuli locations along the precentral gyrus were elicited with 105% RMT for the upper and with 130%–150% RMT for the lower extremity (C) and then exported into our fiber tracking software iPlan 3.0 as region of interests with a radius of 3 mm (visualized as yellow balls in H and I). The second ROI was seeded in one layer of the caudal pons (E) where the blue color in the color-coded FA-map represents the anterior-posterior pontine course of the pyramidal tract (D and F). Finally, FT was performed with 75% FAT where the tumor is colored in red, the CST of the upper extremity in blue and the CST of the lower extremity in green (G, H, I). In this case, we would recommend the use of IOM – especially during the ventral tumor debulking because the tumor seems to begin infiltrating the CST (G).

2.7. Preoperative evaluation and surgical procedure

The surgical planning and the implementation of nTMS-data into the presurgical workflow have been outlined in detail elsewhere (Rosenstock et al., 2016). In short, the visualization of the motor cortex defined by nTMS positive spots and the tracked CST was made available as 3D reconstruction via the hospital's intranet for preoperative planning and for intraoperative control either on the navigational screen or by projection into the microscope view. A detailed analysis of the spatial relationship between tumor-suspected tissue and eloquent brain region had been performed following a recently published risk stratification model where a critical tumor location is defined by infiltration of the motor cortex or/and subcortical approximation to the CST equal or < 8 mm, respectively (Rosenstock et al., 2016). The surgical strategy was tailored to the individual case – specifically the spatial relation between the tumor and eloquent areas. Intraoperative neurophysiological mapping and monitoring (IOM) was performed as previously described (Frey et al., 2014; Kombos et al., 2009a; Kombos et al., 2009b) where the following IOM phenomena were assessed as warning criteria: persistent MEP amplitude reduction over 50% and reproducible MEPs with subcortical stimulation intensity of 5 mA (Rosenstock et al., 2016). Termination of surgery was at the discretion of the individual surgeon and based on preoperative patient consent, preoperative functional diagnostics, IOM phenomena and general surgical circumstances like blood loss, anesthesiological status etc.

2.8. Statistical analysis

We used descriptive statistics to analyze the patients' characteristics. Data are presented as mean ± standard deviation (SD) in case of

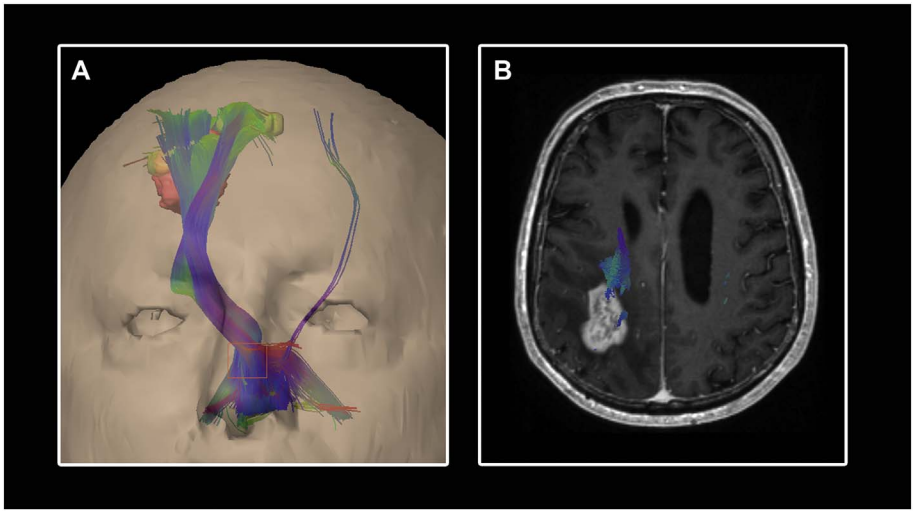

Fig. 2. Illustration of a fiber tracking result using an anatomical-seeded cubic ROI. The same protocol like described in Fig. 1 is used except the second ROI which is placed as orange cubic box in the anterior inferior pons (A). Aberrant fibers, clearly not belonging to the CST, are also visualized. Using this results for planning the surgical resection strategy could lead to an unnecessary restricted resection because aberrant fibers running through the tumor might be preserved by the surgeon (B).

normal distribution or otherwise as median ± interquartile range (IQR), respectively. The unit of the ADC is 10^{-4} mm^2/s and is faded out in the text for reasons of clarity. For testing the relationship between dependent samples, we used the paired *t*-test for normally distributed variables and the Wilcoxon signed-rank test otherwise or the McNemar's test for paired nominal data, respectively. In case of independent samples, testing was performed with the student's *t*-test or the Wilcoxon-Mann-Whitney test, respectively. Correlation testing was performed by using Pearson's correlation coefficient r. To detect significant association between nominal data, we used Fisher's exact test. The interrater reliability analysis was calculated with a two-way random single measure with absolute agreement and presented as mean ± SD or median ± IQR, respectively, for each examiner and intraclass correlation coefficient with 95% confidence intervals.

Analysis of the patients' outcome depending on the diffusion parameters has been performed in two ways: A) motor outcome (deteriorated vs. non-deteriorated motor status) and B) postoperative motor status (existence of a postoperative paresis vs. no postoperative paresis). Additionally, the usefulness of diffusivity parameters for highly significant relations ($p < 0.01$) is demonstrated with ROC analysis (receiver operating characteristics) as area under the curve (AUC) with 95% confidence intervals.

The level of significance was 0.05 (2 sided). Data analysis was performed using SPSS (IBM SPSS Statistics version 22, IBM Corp.).

3. Results

3.1. Patients sample

Thirty patients with high grade glioma in or associated to motor eloquent areas were prospectively enrolled for preoperative motor mapping followed by nTMS-based DTI FT of the CST for both hemispheres. The patients' characteristics are given in Table 1. Two of three patients were under antiepileptic medication and 12 patients (40%) received dexamethasone against edema.

Table 1
Demographic and clinical characteristics of the patients.

	Patients
Age [years]	55 ± 16
Sex	
Male	20 (67%)
Female	10 (33%)
Preoperative motor status	
Paresis	16 (53%)
No paresis	14 (47%)
KPS	
≤ 70%	7 (23%)
80%	5 (17%)
90%	10 (33%)
100%	8 (27%)
Affected hemisphere	
Right	10 (33%)
Left	20 (67%)
Tumor localization	
M1	11 (37%)
M2	7 (23%)
Subcortical	9 (30%)
Other	3 (10%)
Tumor histology	
WHO III	4 (13%)
WHO III (rec.)	1 (3%)
WHO IV	23 (77%)
WHO IV (rec.)	2 (7%)
Tumor volume [ml]	29 ± 24
Edema within CST	
Yes	11 (37%)
No	19 (63%)

Detailed overview on age (presented as mean ± SD), sex, preoperative motor status, KPS = Karnofsky performance score, tumor localization, histology (rec. = recurrent) and volume (presented as median ± IQR) and presence of edema. M1 = tumor infiltrates the motor cortex and approximates ≤ 8 mm to the CST, M2 = tumor seems to "touch" the motor cortex but does not infiltrate it nor approximate to CST ≤ 8 mm, subcortical = tumor is subcortically located and approximates ≤ 8 mm to the CST, other = tumor is not infiltrating or touching the motor cortex nor approximates ≤ 8 mm.

3.2. Navigated TMS mapping

No seizures or persistent side effects were observed during the brain mapping. One patient (3%) complained about headache after the mapping which disappeared within 1 h. The primary motor cortex could be identified in all cases. The mean resting motor threshold (RMT) for the affected hemisphere was 59.3 V/m ± 15.4 and for the healthy hemisphere was 63.1 V/m ± 13.4. The median amplitude of the MEPs (elicited with a stimulation intensity equivalent to the RMT) was 173 μV ± 253 for the affected hemisphere and 222 μV ± 576 for the healthy hemisphere. The mean latency of the MEPs was 23.9 ms ± 1.8 for the tumorous hemisphere and 24.2 ms ± 1.6 for the other hemisphere.

Presence of edema within the CST decreases the mean RMT on the affected hemisphere (51 V/m ± 11.1 vs. 64 V/m ± 15.8, $p = 0.024$) and decreases the median amplitude of the MEP on the healthy hemisphere (120.4 μV ± 124.9 vs. 342.8 μV ± 588.2, $p = 0.006$) whereas

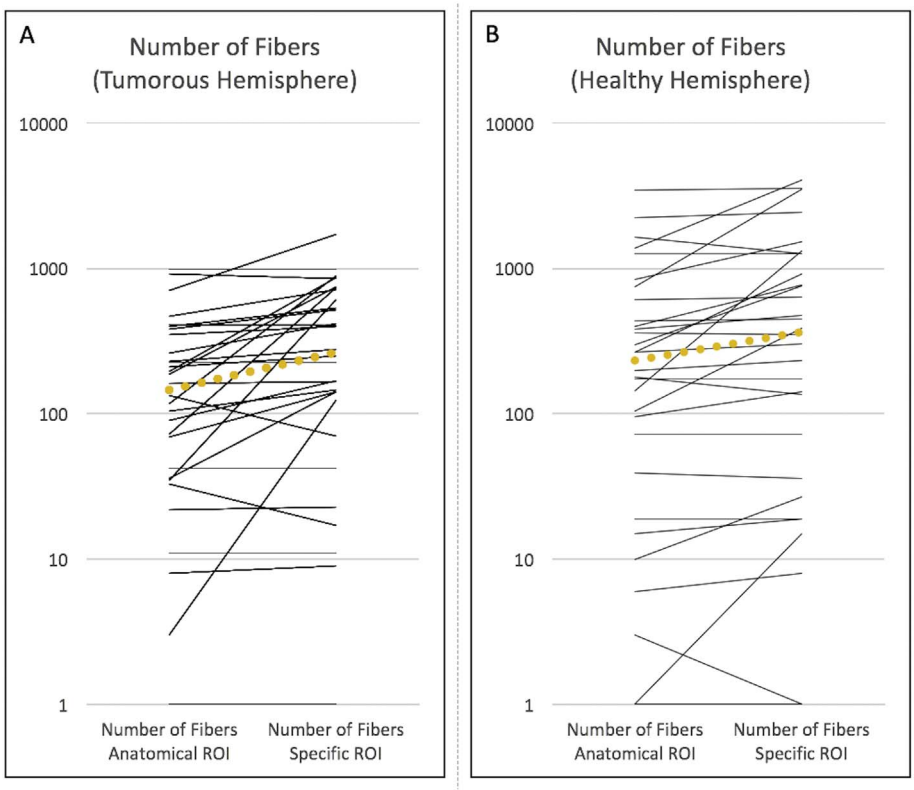

Fig. 3. Comparison of the number of fibers produced by DTI FT of the CST with a cubic anatomical ROI and a specific ROI based on the color-coded FA-map for A) the tumorous hemisphere and B) for the healthy hemisphere. Each line represents one patient's number of fibers where the yellow spotted lines visualize the medians. The use of a specific ROI increases the number of CST-fibers by 180% for the tumorous hemisphere and by 160% for the healthy hemisphere.

no other significant association between presence of edema and neurophysiological parameters could be found (data not shown).

3.3. Comparison of cubic-anatomical vs. specific-FA-based ROI

Navigated TMS-based FT was successfully performed in all patients bihemispherically. The estimated FAT did not differ between the two approaches but between the affected hemisphere (mean FAT for cubic-anatomical approach 0.24 ± 0.08, mean FAT for specific-FA-based approach 0.24 ± 0.08, $p = 0.452$) and healthy hemisphere (mean FAT for cubic-anatomical approach 0.30 ± 0.09, mean FAT for specific-FA-based approach 0.28 ± 0.09, $p = 0.136$) (p-value for interhemispheric comparison: $p = 0.021$ with cubic-anatomical approach, $p = 0.057$ with specific-FA-based approach).

The median number of fibers within the CST could be increased by 180% for the tumorous hemisphere ($p < 0.001$) and by 160% for the healthy hemisphere ($p = 0.001$) by using the specific-FA-based ROI instead of the cubic-anatomical ROI (Fig. 3). Although the median number of tracked fibers is higher on the healthy hemisphere for both subcortical ROIs (Fig. 3), this did not reach statistical significance (cubic-anatomical ROI $p = 0.106$, specific-FA-based ROI $p = 0.371$). The presence of edema within the tumorous CST results in a lower FA-value (see below) and in more producible tracts – independent from the use of a specific-FA-based ROI (median 752 ± 645 vs. 147 ± 364, $p = 0.001$) or a cubic-anatomical ROI (median 197 ± 588 vs. 90 ± 239, $p = 0.057$).

Aberrant fibers (= clearly not belonging to the CST) occurred in 24 patients (80%) in the affected hemisphere and in 22 patients (73%) in the healthy hemisphere when using a cubic-anatomical ROI. In contrast, FT with the specific-FA-based ROI let to appearance of aberrant fibers in just one patient (3%) for both hemispheres (affected hemisphere and healthy hemisphere respectively $p < 0.001$). The median number of aberrant fibers tracked with the cubic-anatomical ROI was 30.5 ± 109 for the tumorous hemisphere and 38 ± 118 for the other hemisphere.

The comparison of the measured closest distance between tumor and CST did not show a significant difference depending on the use of a cubic-anatomical ROI (median 7.0 mm ± 11.25) or specific-FA-based ROI (median 6.75 ± 9.13) ($p = 0.762$).

3.4. Analysis of the FA and ADC value measured within the CST

The measured average FA value within the CST was lower in the tumorous hemisphere compared to the healthy hemisphere (Table 2, $p = 0.001$) – independent from the use of a FA-based or anatomical-seeded ROI (healthy hemisphere Pearson's $r = 0.909$ $p < 0.001$, affected hemisphere Pearson's $r = 0.961$ $p < 0.001$). A decreased average FA value in the tumorous hemisphere was detected when edema was present within the CST (0.44 ± 0.06 vs. 0.48 ± 0.04, $p = 0.045$).

Similarly, a strong accordance in terms of average ADC values within the CST could be found when comparing both approaches (healthy hemisphere Pearson's $r = 0.890$, $p < 0.001$; affected hemisphere Pearson's $r = 0.867$, $p < 0.001$) but the median ADC value was higher in the tumorous hemisphere compared to the healthy hemisphere (Table 2, $p = 0.002$). Edema also influenced the average ADC value in the affected hemisphere (edema present: 25.3 ± 3.02, edema not present: 23.7 ± 2.76, $p = 0.010$).

The spatial changes of the diffusion parameters within the CST are presented in an absolute and relative manner for both hemispheres in Table 2. Comparison of the FA value at the mesencephal level and the peritumoral level in the tumorous hemisphere revealed a mean peritumoral decrease of 0.22 for the FA value as could be expected ($p < 0.001$). A similar but inverse correlation could be found for the ADC value in patients with edema within the CST but not reached statistical significance (Table 2). Moreover, significant interhemispheric differences were detected for both, the FA and ADC value, at the peritumoral level and in average (Table 2). The greater the closest distance between tumor and CST was the higher was the peritumoral FA value (Pearson's $r = 0.594$, $p < 0.001$, Fig. 4) but no other

Table 2
Spatial analysis of the diffusion parameters (FA and ADC) within the CST.

Parameter/location	Affected hemisphere		Healthy hemisphere		Interhemispheric ratio (aff./heal.)	p-Value
	Absolute	Relative	Absolute	Relative		
FA						
Average	0.46 ± 0.05	1	0.51 ± 0.04	1	90%	**0.001**
"Cortical"	0.26 ± 0.09	57%	0.31 ± 0.09	61%	84%	0.605
Peritumoral	0.40 ± 0.13	87%	0.46 ± 0.11	90%	87%	**0.036**
/edema	0.34 ± 0.09	74%				
\edema	0.44 ± 0.14	96%				
Mesencephal	0.62 ± 0.08	135%	0.62 ± 0.11	122%	100%	0.988
Pontine	0.43 ± 0.10	93%	0.47 ± 0.12	92%	91%	0.154
ADC [10^{-4} mm^2/s]						
Average	24.47 ± 4.09	1	23.12 ± 2.36	1	106%	**0.002**
"Cortical"	21.36 ± 4.75	87%	20.52 ± 3.38	89%	104%	0.221
Peritumoral	23.42 ± 5.45	96%	21.80 ± 2.04	94%	107%	**0.001**
/edema	27.32 ± 8.22	112%				
\edema	22.88 ± 4.46	94%				
Mesencephal	24.59 ± 6.37	100%	25.55 ± 3.89	111%	96%	0.441
Pontine	20.95 ± 4.39	86%	21.89 ± 3.57	95%	96%	0.339

Detailed overview on FA (presented as mean ± SD) and ADC values (presented as median ± IQR) measured in different locations based on specific-FA-based ROI. "Cortical" = most cranial part of the CST. /edema = edema was present within the CST. \edema = edema was not present within the CST. The column of relative values allows to identify easily locations where the corresponding value is higher or lower than in average. An interhemispheric ratio of the absolute values was calculated to analyze differences between the tumorous and the healthy hemisphere in detail. Statistic shows that both the FA and ADC value differs significantly ($p < 0.05$) at the peritumoral level (and in average) between the hemispheres.

significant relation could be found in terms of tumor-tract-distance and diffusion parameters (data not shown). When analyzing this correlation without the outlier (#7), there is still a significant correlation (Pearson's $r = 0.390$, $p = 0.036$). In terms of presence of edema, equal effects like described above for the average values could be investigated for the peritumoral values (Table 2).

Correlation analysis of FA and ADC values shows an inverse correlation in average (Pearson's $r = -0.463$, $p = 0.010$), peritumoral (Pearson's $r = -0.496$, $p = 0.005$) and mesencephal (Pearson's $r = -0.748$, $p < 0.001$).

3.5. Analysis of different adjusted FA-values

DTI FT was also performed with the same specific-FA-based ROIs but different adjusted FA-values for all patients. When decreasing the adjusted FA-value lower than 75% FAT, the incidence of aberrant fibers increases and consequently the rate of plausible fiber tracking results is lower (Table 3).

3.6. Interrater reliability analysis

The unexperienced as well as the other experienced examiner performed a plausible fiber tracking of the CST in all patients. When analyzing the continuous variables of the examiners' fiber tracking, a significant perfect agreement (ICC > 0.8) could be reached for nearly all parameters – except the average volume of the CST where a moderate agreement (ICC > 0.5) could be verified (Table 4). No additional aberrant fibers occurred in the FTs of the other raters which means an absolute agreement of 97%. The measured closest distance between tumor and CST – as the clinically most relevant variable of the interrater reliability analysis – is also visualized in Fig. 5.

3.7. Patients outcome

Analysis of the spatial relationship between tumor and eloquent tissue based on nTMS-mapping and nTMS-based FT revealed a critical tumor location in 20 patients (67%). Eight patients of them suffered from a paresis that did not recover over time whereas no patient deteriorated postoperatively whose tumor location had been determined as uncritical (outcome day of discharge $p = 0.029$, outcome after 3 months, $p = 0.027$). In contrast, 4 patients (13%) could improve their motor status examined on day of discharge and one more regained motor function after 3 months. One patient (3%) did not attend to the follow-up date after 3 months (reason unknown).

Six (55%) out of 11 patients, in which edema was detected within the CST, got worse in terms of motor function postoperatively versus 2 (11%) out of 19 patients without edema (outcome day of discharge $p = 0.028$, outcome after 3 months $p = 0.009$).

A decreased average FA value is associated with postoperative deterioration of motor function at the day of discharge ($p = 0.007$, AUC = 0.790 [0.619–0.960] $p = 0.017$) as well as after 3 months ($p = 0.006$, AUC = 0.804 [0.639–0.968] $p = 0.013$) (Fig. 6). A lower peritumoral FA value (means 0.37 ± 0.12 vs. 0.45 ± 0.14, $p = 0.110$) as such but also its relative decrease in comparison to the

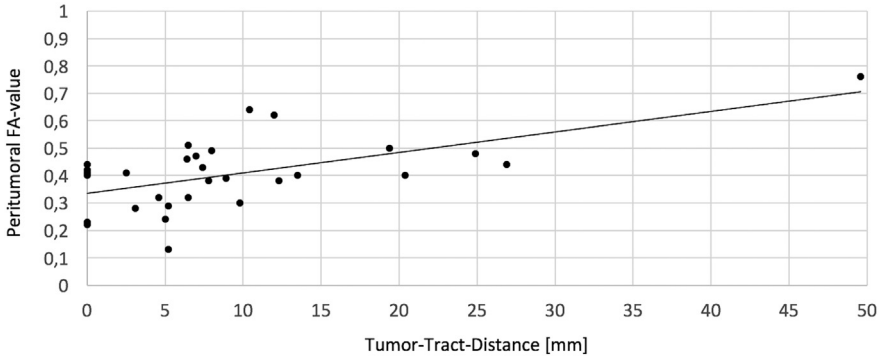

Fig. 4. Visualization of the relationship between the tumor-tract-distance and the peritumoral FA-value. Correlation analysis confirms that there is a significant correlation between the distance and the peritumoral FA-value (Pearson's $r = 0.594$, $p < 0.001$) – even if the outlier is excluded when calculating Pearson's r (Pearson's $r = 0.390$, $p = 0.036$).

Table 3
Data from CST-FT depending on different adjusted FA-values.

Adjusted FA-value	Plausible FT	Number of fibers	Occurrence of aberrant fibers	Average fiber length [mm]	Tract volume [ml]	Average FA-value within CST	Average ADC-value within CST [$mm^2/s \cdot 10^{-4}$]	Closest distance measured between tumor and CST [mm]
0.01	22 (73%)	1755 ± 2326	26 (87%)	134 ± 18.50	14.13 ± 9.09	0.41 ± 0.05	27.68 ± 4.95	5.3 ± 8.38
0.05	26 (87%)	1743 ± 2431	22 (73%)	130.5 ± 20.63	12.12 ± 7.55	0.42 ± 0.04	27.72 ± 30.01	5.3 ± 8.38
0.10[a]	28 (100%)	1135 ± 1884	16 (53%)	126 ± 20.25	8.10 ± 4.63	0.44 ± 0.05	25.71 ± 4.42	6.3 ± 10.88
25% FAT	28 (93%)	1466 ± 2206	21 (70%)	130 ± 21.12	10.98 ± 6.87	0.42 ± 0.05	26.72 ± 5.16	5.65 ± 8.38
50% FAT	30 (100%)	1025 ± 1322	12 (40%)	122 ± 20.80	6.66 ± 4.06	0.44 ± 0.05	25.04 ± 3.99	6.25 ± 10.0
75% FAT	30 (100%)	279 ± 576	1 (3%)	120.5 ± 19.0	3.41 ± 1.89	0.46 ± 0.05	24.47 ± 4.95	6.75 ± 9.13

Detailed overview on the dependency of the adjusted FA-value on the FT parameters. CST = corticospinal tract, FAT = fractional anisotropy threshold, FT = fiber tracking. The number of fibers, the average fiber length, the ADC value within the CST and the closest distance between tumor and CST are presented as median ± IQR. The tract volume and the average FA-value within the CST are presented as mean ± SD.

[a] In 2 patients, no FT could be performed with an adjusted FA-value of 0.10 because the FAT was lower than 0.10.

mesencephal level (Fig. 6) showed a relationship with postoperative impaired motor function (= existence of a postoperative paresis) on day of discharge, but without statistical significance.

Higher ADC values within the CST of the tumorous hemisphere, measured in average (p = 0.026, Fig. 6) or especially at the peritumoral level (median 25.0 ± 8.48 vs. 22.9 ± 3.41, p = 0.038), are correlated to an affected motor status at day of discharge. When analyzing the course within the CST, a peritumoral increase of the ADC value compared to the mesencephal level is also associated with an affected motor status at day of discharge (p = 0.002, AUC = 0.796 [0.629–0.967] p = 0.007) and after 3 months (p = 0.007, AUC = 0.719 [0.525–0.913] p = 0.045) (Fig. 6) and is positively correlated with postoperative deterioration of motor function (day of discharge: mean difference in deteriorated patients = 2.29 ± 6.60 vs. non-deteriorated patients = −2.13 ± 6.04, p = 0.094; after 3 months: mean difference in deteriorated patients = 2.29 ± 6.60 vs. non-deteriorated patients = −2.54 ± 5.87, p = 0.066). The comparison of the two hemispheres at the peritumoral level revealed that higher ADC values on the tumorous hemisphere are related to an affected postoperative motor status (day of discharge: median difference in paretic patients = 3.40 ± 6.86 vs. nonparetic patients = 0.97 ± 3.15, p = 0.047; after 3 months: median difference in paretic patients = 2.66 ± 7.00 vs. nonparetic patients = 1.49 ± 3.49, p = 0.150). Moreover, the interhemispheric peritumoral difference of the ADC predicted the postoperative motor outcome (day of discharge: median difference in deteriorated patients = 4.61 ± 9.91 vs. non-deteriorated patients = 1.58 ± 3.86, p = 0.133; after 3 months: median difference in deteriorated patients = 4.61 ± 9.91 vs. non-deteriorated patients = 1.55 ± 3.71, p = 0.088).

4. Discussion

4.1. Background

In patients with affected CST (e.g. by gliomas), utilizing of nTMS data as seed region for the FT procedure is superior to conventional FT which only bases on anatomical landmarks. In detail, the insertion of nTMS data allows to visualize especially perilesional fibers and therefore enriches the preoperative planning and intraoperative orientation (Forster et al., 2015; Frey et al., 2012; Krieg et al., 2012a). Moreover, a distance between tumor and DTI-derived CST equal or < 8 mm has been determined as negative predictor in terms of postoperative motor function which allows to identify high risk cases where intraoperative neuromonitoring with subcortical stimulation is strongly advised (Rosenstock et al., 2016). On the other hand, a tumor-tract-distance < 8 mm not necessarily leads to the occurrence of a new paresis. Based on our data, the diffusion parameters can be used as additional parameters to estimate more precisely the risk of postoperative functional deterioration.

Since the first description of implementing nTMS-data as seed region into the tracking algorithm by Krieg et al. (2012a), different additional subcortical ROIs were used where the best available tracking results for the CST had been reached with an anatomically seeded cubic ROI in the pons (Weiss et al., 2015). There are some studies suggesting

Table 4
Interrater reliability results for the FT parameters.

Parameter	Mean ± SD or median ± IQR			ICC (p value)	95% CI
	Rater A	Rater B	Rater C		
Affected hemisphere					
Number of fibers	264 ± 615	255 ± 574	141 ± 469	0.868 (< 0.001)	0.76–0.93
FAT[a]	0.24 ± 0.08	0.23 ± 0.08	0.23 ± 0.08	0.982 (< 0.001)	0.97–0.99
Average FA[a]	0.46 ± 0.05	0.46 ± 0.05	0.47 ± 0.05	0.951 (< 0.001)	0.91–0.98
Average length[b]	120.5 ± 19.0	117 ± 18.25	119 ± 14.75	0.966 (< 0.001)	0.94–0.98
Average volume [cm^3][a]	3.41 ± 1.89	3.20 ± 1.58	4.75 ± 3.53	0.651 (< 0.001)	0.37–0.82
Average ADC [$mm^2/s \cdot 10^{-4}$][b]	24.47 ± 4.09	24.43 ± 3.0	25.20 ± 3.86	0.958 (< 0.001)	0.92–0.98
Distance CST ~ tumor [mm][b]	6.75 ± 9.13	7.4 ± 9.50	7.2 ± 8.78	0.993 (< 0.001)	0.99–1.0
Healthy hemisphere					
Number of fibers[b]	369 ± 1232	363 ± 1170	333 ± 1181	0.935 (< 0.001)	0.88–0.97
FAT[a]	0.28 ± 0.09	0.29 ± 0.09	0.29 ± 0.09	0.973 (< 0.001)	0.95–0.99
Average FA[a]	0.51 ± 0.04	0.51 ± 0.05	0.51 ± 0.05	0.937 (< 0.001)	0.89–0.97
Average length[b]	118 ± 11.75	118.5 ± 12.75	116.5 ± 11.0	0.957 (< 0.001)	0.92–0.98
Average volume [cm^3][a]	3.12 ± 1.50	2.80 ± 1.36	4.30 ± 3.52	0.586 (0.001)	0.27–0.79
Average ADC [$mm^2/s \cdot 10^{-4}$][b]	23.12 ± 1.74	23.20 ± 2.30	23.35 ± 2.92	0.958 (< 0.001)	0.92–0.98

Detailed comparison of the examiners' results where rater A and B are experienced and rater C is unexperienced.

[a] Data is presented as mean ± SD.

[b] Data is presented as median ± IQR.

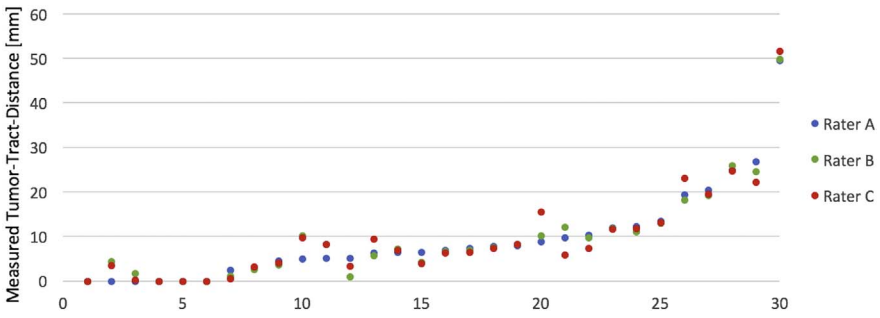

Fig. 5. Visualization of the closest distance between tumor and CST measured by two experienced (rater A and B) and one unexperienced examiner (rater C). Interrater reliability analysis confirms a perfect agreement (ICC = 0.993, $p < 0.001$).

that nTMS-based DTI FT is less user-dependant than conventional DTI FT of the CST (Conti et al., 2014; Frey et al., 2012; Krieg et al., 2012a) but no interrater reliability analysis of the tracking results was performed yet.

Although fMRI-derived ROI seeding for the visualization of the corticospinal tract has been described (Smits et al., 2007), it has been criticized – especially in patients suffering from a malignant brain tumor – because of tumor's mass effect and neurovascular decoupling effects leading to a methodological inaccuracy (Rutten and Ramsey, 2010). A recently published study could show that nTMS-based DTI FT of the CST is superior in terms of tracking quality and plausibility in patients with a brain tumor in the vicinity of the primary motor area compared to fMRI-based approaches (Weiss Lucas et al., 2017). Thus, the authors recommended the use of the nTMS-technique to identify seed regions.

4.2. Interrater reliability analysis

This is the first study comparing the results of nTMS-based DTI-derived CST between two experienced and a novice examiner. We want to highlight that a perfect agreement (ICC > 0.8) could be reached for all analyzed parameters (except the tract volumes with at least moderate agreement [ICC > 0.5]) with highly statistical significance. Particularly, the very high reliability of the measured tumor-tract-distance might be the most important result because it is the crucial parameter for evaluating in how far gross total resection is feasible without an increased risk for functional deterioration. Thus, nTMS-based FT can be used to support the surgical strategy planning and patient counseling in cases with brain tumors in a user-independent and highly reliable manner without the necessity of an expert user.

4.3. Specific ROI seeding in the color-coded FA-map

Weiss et al. have been recently shown that an additional anatomical-seeded cubic ROI beside the nTMS-based ROI can increase the feasibility rates of DTI FT of the ipsilesional CST up to 94% for the upper and in 81% for the lower extremity (Weiss et al., 2015).

The specific ROI seeding for DTI FT of the CST based on color-coded FA maps in the caudal pons in patients with glioma affecting the motor system has been described for the first time in the present study (Fig. 1). A plausible FT of the CST could be performed in each patient for both the upper and lower extremity with the specific ROI. Moreover, the FT with the specific ROI reveals more CST fiber bundles which had been judged as plausible by our interdisciplinary board of neurosurgeons and neuroradiologists. On the other hand, the specific ROI reduces the prevalence of aberrant fibers (rater A: 3%, rater B and C: 0%) and allows an improved analysis of the spatial relationship between functional tissue and tumor.

In this study, we used the FA thresholding algorithm of Frey et al. (2012), but we also performed FT with different adjusted FA values in a dense raster. When decreasing the adjusted FA value under 75% FAT, the plausibility rate is not longer 100% where aberrant fibers appeared

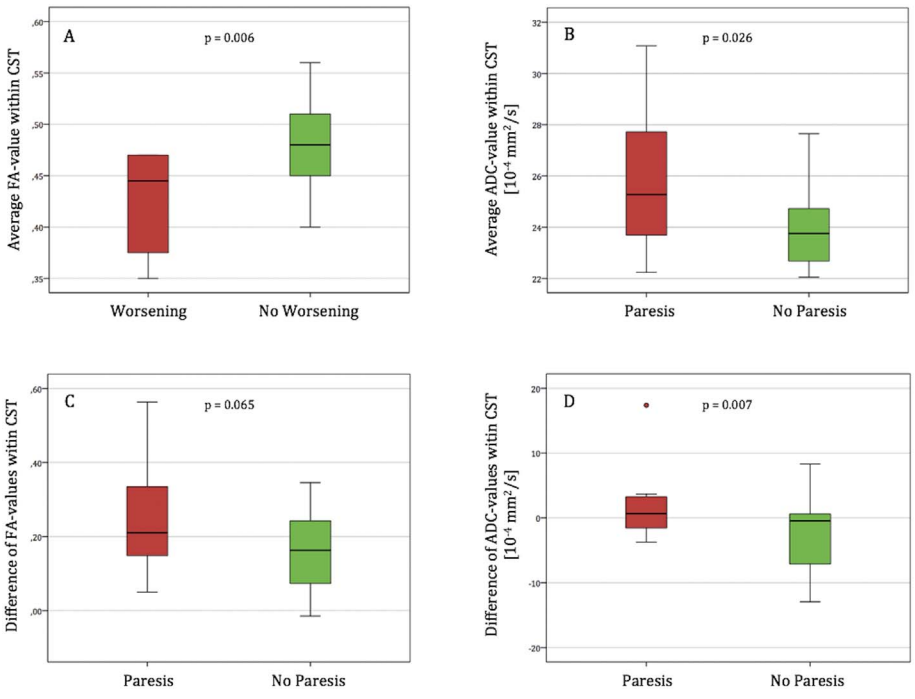

Fig. 6. Box plots illustrating the distribution of the diffusion parameters and their intrahemispheric difference between the mesencephal and the peritumoral level, according to the postoperative motor outcome or status, respectively. Lower average FA-values within the tumorous CST (A) are significantly associated with postoperative deterioration of the motor system after 3 months. An existing motor deficit on day of discharge is in relation to higher average ADC-values within the tumorous CST (B). Comparison of the diffusion parameters in different locations (mesencephal vs. peritumoral) revealed that high differences could be especially found in patients with an impaired motor status on day of discharge (C) or after 3 months (D), respectively.

more often. In Addition, the tumor-tract-distance decreases and might lead to inadequate interpretation of tracking results. Therefore we advise to follow the established thresholding and to not lower the adjusted FA value under 75% FAT when performing DTI FT of the CST.

The results of the interrater reliability analysis and the comparison of anatomical vs. color-coded FA-map ROI seeding suggest that our standardized procedure increases the tracking quality and seems to be superior towards tracking algorithms published so far.

4.4. Diffusivity parameters and edema

This is the first study analyzing the FA and ADC value within the nTMS-based DTI-derived CST in different locations in patients with glioma approximating the CST.

We could show that the FA value is lower and the ADC value is higher in the affected hemisphere – especially at the peritumoral level. This finding goes in line with two other studies presenting a similar interhemispheric difference for the FA value within a non-functional DTI-derived CST in patients with subcortical glioma (Giordano et al., 2015; Stadlbauer et al., 2007). Moreover, there are current meta-analyses of DTI studies suggesting that decreased FA values caused by different neurological diseases (e.g. ischemic stroke, intracerebral hemorrhage, Huntington's disease) are associated with an affected motor status (Chen et al., 2016; Kumar et al., 2016a; Kumar et al., 2016b; Liu et al., 2016). Just one study previously showed in patients with various brain tumor entities, that an affected preoperative motor status seems to be in relationship with interhemispheric differences of the FA and ADC value based on non-functional DTI-derived CSTs (Bobek-Billewicz et al., 2011). This fits well with our findings that interhemispheric differences of the diffusivity parameters can be used preoperatively to predict the postoperative motor outcome. In addition, the comparison of the diffusivity parameters at different locations revealed that the FA and ADC value are especially affected at the peritumoral level of the tumorous hemisphere only. Consequently, no significant interhemispheric difference in terms of diffusivity could be found elsewhere.

It is widely known that tracking results are often impaired in patients with brain tumors by tumor mass effects and perilesional edema because anisotropic diffusivity is disturbed (Mandelli et al., 2014; Schonberg et al., 2006; Zolal et al., 2013). The peritumoral decrease of the FA value and increase of the ADC value found in our patients – especially when edema was present – go in line with the current state of research (Lu et al., 2003), however the spatial specific impairment of the diffusivity parameters at the peritumoral level has been examined for the first time.

One study showed that nTMS is sometimes not feasible when (excessive) edema is present (Conti et al., 2014). In contrast, we could elicit MEPs in all our patients with RMT values of the tumorous hemisphere being significant lower in patients with edema within the CST. Sollmann et al. could show an equal decrease of the RMT for tumorous edematous hemispheres in patients with various tumor entities and described this phenomenon as increased excitability caused by decreased plasma osmolality (Sollmann et al., 2017). Following this hypothesis, an increased excitability of the tumorous hemisphere could explain lower healthy hemisphere MEP amplitudes caused by interhemispheric inhibition (Davidson and Tremblay, 2013; Perez and Cohen, 2009). A better permeability of the induced e-field due to the edema may also explain the decreased RMT of the tumorous hemisphere.

Another study reported that presence of edema lead to implausible FT results (Weiss et al., 2015). In our patients, a plausible FT could be performed in each case where aberrant fibers just occurred in one case. In the present study, the presence of edema rather resulted in a higher number of fibers belonging to the CST and might confirm our opinion that the presented nTMS-based FT procedure is a robust method for evaluating in how far the tumor location is risky in terms of postoperative motor deterioration – even if peritumoral edema is present within the course of the CST. It needs to be stressed that a strong correlation between the presence of edema within the CST and an impaired postoperative motor status was observed in our study.

Further research is needed to better understand in how far edema and intracortical/interhemispheric excitation-inhibition-balancing influence the motor system's functionality in patients with brain lesions. Moreover, prospective study's attention should be payed especially to the peritumoral level when analyzing the DTI-derived CST in brain tumor patients. It is remarkable that an impaired postoperative motor status correlates with the extent of diffusivity-disturbance within the tumorous CST (peritumoral vs. mesencephal level).

4.5. Limitations

All presented results of this study are based on a consecutive cohort of 30 patients treated in our department. Thus, we cannot exclude that our results were influenced by the specific decision-making processes and treatment algorithms of our department.

Although there are some studies suggesting that better tracking results of the CST can be reached with probabilistic FT (Bucci et al., 2013; Mandelli et al., 2014) instead of deterministic approaches, no comparison between nTMS-based FT results have been published in this respect yet. Also, the main advantage of probabilistic FT with voxel deconvolution is claimed for its robustness against edema – in our study deterministic DTI FT was successful despite the presence of edema in all cases. Seeding of specific functional ROIs in motor-associated tumor locations is essential for evaluating the spatial relationship between eloquent area and tumorous tissue because this is the only method to reliably account for tumor-induced neuronal plasticity and rearrangement of the motor pathway (Duffau, 2007; Krieg et al., 2012a; Lehericy et al., 2000) which cannot be considered when just using anatomical landmarks. Furthermore, deterministic FT is more time-efficient and more useful in clinical context when treating and counseling patients where standardized procedures are required.

The accuracy of the nTMS-based FT has been recently shown (Forster et al., 2015) and all tracking results were critically analyzed by our interdisciplinary board including neurosurgeons and neuroradiologists. Nevertheless, the number of fibers as a parameter to assess the quality of tractography is a weak and controversial measure. Moreover, a validation of the fibers in brain tumor patients by subcortical stimulation is challenging due to brain shift and electrical current spread.

5. Conclusions

Navigated TMS-based motor DTI not only offers data for analyzing the spatial relationship between tumor and functionally essential tissue but also provides information on the structural integrity of the tracts, which improves the patient counseling and the prediction of postoperative motor outcome. A second subcortical ROI, specifically seeded based on the color-coded FA map, increases the tracking quality of the CST and is highly reliable – independently of the examiner's experience.

Further prospective studies are needed to validate the nTMS-based prediction of the patient's outcome.

References

Almenawer, S.A., Badhiwala, J.H., Alhazzani, W., Greenspoon, J., Farrokhyar, F., Yarascavitch, B., Algird, A., Kachur, E., Cenic, A., Sharieff, W., Klurfan, P., Gunnarsson, T., Ajani, O., Reddy, K., Singh, S.K., Murty, N.K., 2015. Biopsy versus partial versus gross total resection in older patients with high-grade glioma: a systematic review and meta-analysis. Neuro Oncol. 17, 868–881.

Basser, P.J., Mattiello, J., LeBihan, D., 1994. MR diffusion tensor spectroscopy and imaging. Biophys. J. 66, 259–267.

Bobek-Billewicz, B., Stasik-Pres, G., Majchrzak, K., Senczenko, W., Majchrzak, H., Jurkowski, M., Poletek, J., 2011. Fibre integrity and diffusivity of the pyramidal tract and motor cortex within and adjacent to brain tumour in patients with or without neurological deficits. Folia Neuropathol. 49, 262–270.

Bucci, M., Mandelli, M.L., Berman, J.I., Amirbekian, B., Nguyen, C., Berger, M.S., Henry,

R.G., 2013. Quantifying diffusion MRI tractography of the corticospinal tract in brain tumors with deterministic and probabilistic methods. Neuroimage Clin. 3, 361–368.
Chen, L., Hu, X., Ouyang, L., He, N., Liao, Y., Liu, Q., Zhou, M., Wu, M., Huang, X., Gong, Q., 2016. A systematic review and meta-analysis of tract-based spatial statistics studies regarding attention-deficit/hyperactivity disorder. Neurosci. Biobehav. Rev. 68, 838–847.
Conti, A., Raffa, G., Granata, F., Rizzo, V., Germano, A., Tomasello, F., 2014. Navigated transcranial magnetic stimulation for "somatotopic" tractography of the corticospinal tract. Neurosurgery 10 (Suppl. 4), 542–554.
Davidson, T., Tremblay, F., 2013. Hemispheric differences in corticospinal excitability and in transcallosal inhibition in relation to degree of handedness. PLoS One 8, e70286.
Duffau, H., 2007. Contribution of cortical and subcortical electrostimulation in brain glioma surgery: methodological and functional considerations. Neurophysiol. Clin. 37, 373–382.
Duffau, H., Lopes, M., Arthuis, F., Bitar, A., Sichez, J.P., Van Effenterre, R., Capelle, L., 2005. Contribution of intraoperative electrical stimulations in surgery of low grade gliomas: a comparative study between two series without (1985–96) and with (1996–2003) functional mapping in the same institution. J. Neurol. Neurosurg. Psychiatry 76, 845–851.
Forster, M.T., Hattingen, E., Senft, C., Gasser, T., Seifert, V., Szelenyi, A., 2011. Navigated transcranial magnetic stimulation and functional magnetic resonance imaging: advanced adjuncts in preoperative planning for central region tumors. Neurosurgery 68, 1317–1324 (discussion 1324-1315).
Forster, M.T., Limbart, M., Seifert, V., Senft, C., 2014. Test-retest reliability of navigated transcranial magnetic stimulation of the motor cortex. Neurosurgery 10 (Suppl. 1), 51–55 (discussion 55-56).
Forster, M.T., Hoecker, A.C., Kang, J.S., Quick, J., Seifert, V., Hattingen, E., Hilker, R., Weise, L.M., 2015. Does navigated transcranial stimulation increase the accuracy of tractography? A prospective clinical trial based on intraoperative motor evoked potential monitoring during deep brain stimulation. Neurosurgery 76, 766–776.
Frey, D., Strack, V., Wiener, E., Jussen, D., Vajkoczy, P., Picht, T., 2012. A new approach for corticospinal tract reconstruction based on navigated transcranial stimulation and standardized fractional anisotropy values. NeuroImage 62, 1600–1609.
Frey, D., Schilt, S., Strack, V., Zdunczyk, A., Rosler, J., Niraula, B., Vajkoczy, P., Picht, T., 2014. Navigated transcranial magnetic stimulation improves the treatment outcome in patients with brain tumors in motor eloquent locations. Neuro-Oncology 16, 1365–1372.
Giordano, M., Nabavi, A., Gerganov, V.M., Javadi, A.S., Samii, M., Fahlbusch, R., Samii, A., 2015. Assessment of quantitative corticospinal tract diffusion changes in patients affected by subcortical gliomas using common available navigation software. Clin. Neurol. Neurosurg. 136, 1–4.
Hervey-Jumper, S.L., Berger, M.S., 2016. Maximizing safe resection of low- and high-grade glioma. J. Neurooncol. 130, 269–282.
Kombos, T., Picht, T., Derdilopoulos, A., Suess, O., 2009a. Impact of intraoperative neurophysiological monitoring on surgery of high-grade gliomas. J. Clin. Neurophysiol. 26, 422–425.
Kombos, T., Suss, O., Vajkoczy, P., 2009b. Subcortical mapping and monitoring during insular tumor surgery. Neurosurg. Focus. 27, E5.
Krieg, S.M., Buchmann, N.H., Gempt, J., Shiban, E., Meyer, B., Ringel, F., 2012a. Diffusion tensor imaging fiber tracking using navigated brain stimulation—a feasibility study. Acta Neurochir. 154, 555–563.
Krieg, S.M., Shiban, E., Buchmann, N., Gempt, J., Foerschler, A., Meyer, B., Ringel, F., 2012b. Utility of presurgical navigated transcranial magnetic brain stimulation for the resection of tumors in eloquent motor areas. J. Neurosurg. 116, 994–1001.
Krieg, S.M., Sabih, J., Bulubasova, L., Obermueller, T., Negwer, C., Janssen, I., Shiban, E., Meyer, B., Ringel, F., 2014. Preoperative motor mapping by navigated transcranial magnetic brain stimulation improves outcome for motor eloquent lesions. Neuro-Oncology 16, 1274–1282.
Kumar, P., Kathuria, P., Nair, P., Prasad, K., 2016a. Prediction of upper limb motor recovery after subacute ischemic stroke using diffusion tensor imaging: a systematic review and meta-analysis. J. Stroke 18, 50–59.
Kumar, P., Yadav, A.K., Misra, S., Kumar, A., Chakravarty, K., Prasad, K., 2016b. Prediction of upper extremity motor recovery after subacute intracerebral hemorrhage through diffusion tensor imaging: a systematic review and meta-analysis. Neuroradiology 58, 1043–1050.
Lehericy, S., Duffau, H., Cornu, P., Capelle, L., Pidoux, B., Carpentier, A., Auliac, S., Clemenceau, S., Sichez, J.P., Bitar, A., Valery, C.A., Van Effenterre, R., Faillot, T., Srour, A., Fohanno, D., Philippon, J., Le Bihan, D., Marsault, C., 2000. Correspondence between functional magnetic resonance imaging somatotopy and individual brain anatomy of the central region: comparison with intraoperative stimulation in patients with brain tumors. J. Neurosurg. 92, 589–598.
Liu, W., Yang, J., Burgunder, J., Cheng, B., Shang, H., 2016. Diffusion imaging studies of Huntington's disease: a meta-analysis. Parkinsonism Relat. Disord. 32, 94–101.
Louis, D.N., Ohgaki, H., Wiestler, O.D., Cavenee, W.K., Burger, P.C., Jouvet, A., Scheithauer, B.W., Kleihues, P., 2007. The 2007 WHO classification of tumours of the central nervous system. Acta Neuropathol. 114, 97–109.
Lu, S., Ahn, D., Johnson, G., Cha, S., 2003. Peritumoral diffusion tensor imaging of high-grade gliomas and metastatic brain tumors. AJNR Am. J. Neuroradiol. 24, 937–941.
Mandelli, M.L., Berger, M.S., Bucci, M., Berman, J.I., Amirbekian, B., Henry, R.G., 2014. Quantifying accuracy and precision of diffusion MR tractography of the corticospinal tract in brain tumors. J. Neurosurg. 121, 349–358.
McGirt, M.J., Mukherjee, D., Chaichana, K.L., Than, K.D., Weingart, J.D., Quinones-Hinojosa, A., 2009. Association of surgically acquired motor and language deficits on overall survival after resection of glioblastoma multiforme. Neurosurgery 65, 463–469 (discussion 469-470).
Mori, S., van Zijl, P.C., 2002. Fiber tracking: principles and strategies - a technical review. NMR Biomed. 15, 468–480.
Negwer, C., Sollmann, N., Ille, S., Hauck, T., Maurer, S., Kirschke, J.S., Ringel, F., Meyer, B., Krieg, S.M., 2016. Language pathway tracking: comparing nTMS-based DTI fiber tracking with a cubic ROIs-based protocol. J. Neurosurg. 1–9.
Negwer, C., Ille, S., Hauck, T., Sollmann, N., Maurer, S., Kirschke, J.S., Ringel, F., Meyer, B., Krieg, S.M., 2017. Visualization of subcortical language pathways by diffusion tensor imaging fiber tracking based on rTMS language mapping. Brain Imaging Behav. 11, 899–914.
Perez, M.A., Cohen, L.G., 2009. The corticospinal system and transcranial magnetic stimulation in stroke. Top. Stroke Rehabil. 16, 254–269.
Picht, T., Mularski, S., Kuehn, B., Vajkoczy, P., Kombos, T., Suess, O., 2009. Navigated transcranial magnetic stimulation for preoperative functional diagnostics in brain tumor surgery. Neurosurgery 65, 93–98 (discussion 98-99).
Picht, T., Schmidt, S., Brandt, S., Frey, D., Hannula, H., Neuvonen, T., Karhu, J., Vajkoczy, P., Suess, O., 2011. Preoperative functional mapping for rolandic brain tumor surgery: comparison of navigated transcranial magnetic stimulation to direct cortical stimulation. Neurosurgery 69, 581–588 (discussion 588).
Picht, T., Frey, D., Thieme, S., Kliesch, S., Vajkoczy, P., 2016. Presurgical navigated TMS motor cortex mapping improves outcome in glioblastoma surgery: a controlled observational study. J. Neuro-Oncol. 126, 535–543.
Rosenstock, T., Grittner, U., Acker, G., Schwarzer, V., Kulchytska, N., Vajkoczy, P., Picht, T., 2016. Risk stratification in motor area-related glioma surgery based on navigated transcranial magnetic stimulation data. J. Neurosurg. 1–11.
Rutten, G.J., Ramsey, N.F., 2010. The role of functional magnetic resonance imaging in brain surgery. Neurosurg. Focus 28, E4.
Sanai, N., Berger, M.S., 2008. Glioma extent of resection and its impact on patient outcome. Neurosurgery 62, 753–764 (discussion 264-756).
Schag, C.C., Heinrich, R.L., Ganz, P.A., 1984. Karnofsky performance status revisited: reliability, validity, and guidelines. J. Clin. Oncol. 2, 187–193.
Schonberg, T., Pianka, P., Hendler, T., Pasternak, O., Assaf, Y., 2006. Characterization of displaced white matter by brain tumors using combined DTI and fMRI. NeuroImage 30, 1100–1111.
Smits, M., Vernooij, M.W., Wielopolski, P.A., Vincent, A.J., Houston, G.C., van der Lugt, A., 2007. Incorporating functional MR imaging into diffusion tensor tractography in the preoperative assessment of the corticospinal tract in patients with brain tumors. AJNR Am. J. Neuroradiol. 28, 1354–1361.
Sollmann, N., Tanigawa, N., Bulubas, L., Sabih, J., Zimmer, C., Ringel, F., Meyer, B., Krieg, S.M., 2017. Clinical factors underlying the inter-individual variability of the resting motor threshold in navigated transcranial magnetic stimulation motor mapping. Brain Topogr. 30, 98–121.
Stadlbauer, A., Nimsky, C., Gruber, S., Moser, E., Hammen, T., Engelhorn, T., Buchfelder, M., Ganslandt, O., 2007. Changes in fiber integrity, diffusivity, and metabolism of the pyramidal tract adjacent to gliomas: a quantitative diffusion tensor fiber tracking and MR spectroscopic imaging study. AJNR Am. J. Neuroradiol. 28, 462–469.
Tarapore, P.E., Tate, M.C., Findlay, A.M., Honma, S.M., Mizuiri, D., Berger, M.S., Nagarajan, S.S., 2012. Preoperative multimodal motor mapping: a comparison of magnetoencephalography imaging, navigated transcranial magnetic stimulation, and direct cortical stimulation. J. Neurosurg. 117, 354–362.
Tarapore, P.E., Picht, T., Bulubas, L., Shin, Y., Kulchytska, N., Meyer, B., Berger, M.S., Nagarajan, S.S., Krieg, S.M., 2016. Safety and tolerability of navigated TMS for preoperative mapping in neurosurgical patients. Clin. Neurophysiol. 127, 1895–1900.
Weiss Lucas, C., Tursunova, I., Neuschmelting, V., Nettekoven, C., Oros-Peusquens, A.M., Stoffels, G., Faymonville, A.M., Jon, S.N., Langen, K.J., Lockau, H., Goldbrunner, R., Grefkes, C., 2017. Functional MRI vs. navigated TMS to optimize M1 seed volume delineation for DTI tractography. A prospective study in patients with brain tumours adjacent to the corticospinal tract. Neuroimage Clin. 13, 297–309.
Weiss, C., Tursunova, I., Neuschmelting, V., Lockau, H., Nettekoven, C., Oros-Peusquens, A.M., Stoffels, G., Rehme, A.K., Faymonville, A.M., Shah, N.J., Langen, K.J., Goldbrunner, R., Grefkes, C., 2015. Improved nTMS- and DTI-derived CST tractography through anatomical ROI seeding on anterior pontine level compared to internal capsule. Neuroimage Clin. 7, 424–437.
Zdunczyk, A., Fleischmann, R., Schulz, J., Vajkoczy, P., Picht, T., 2013. The reliability of topographic measurements from navigated transcranial magnetic stimulation in healthy volunteers and tumor patients. Acta Neurochir. 155, 1309–1317.
Zolal, A., Hejcl, A., Malucelli, A., Novakova, M., Vachata, P., Bartos, R., Derner, M., Sames, M., 2013. Distant white-matter diffusion changes caused by tumor growth. J. Neuroradiol. 40, 71–80.